Article Type: Research

OPEN ACCESS

Enhanced Analysis of Non-Homogeneous Unbounded Soil Media using SBFE Method

Kamyab Abdolnajaghi[1*] , Zahra Abbaspour[1]

[1]Department of Civil Engineering, University of Tabriz, Tabriz 5166616471, Iran
*Corresponding author: kamyab.abd@yahoo.com

Received: 12 July 2024 / Accepted: 22 July 2024 / Published: 25 August 2024

***Abstract*:** Modeling radiation damping effects in wave propagation is complex, and various numerical, analytical, and semi-analytical methods have been proposed to address the problem. The scaled boundary method (SBM) is an efficient semi-analytical approach for analyzing dynamic wave propagation in non-homogeneous, unbounded media. While previous studies often focused on acceleration or displacement unit impulse response-based techniques, this paper introduces a velocity unit impulse response (VUIR)-based SBM for more efficient computation. The authors modified the original VUIR-based SBM formulation to directly derive the dynamic interaction force for non-homogeneous infinite media, bypassing the need to convert velocity responses into displacements. To validate the method, several benchmark numerical examples are solved. The method is shown to be effective in analyzing dynamic wave propagation in both homogeneous and non-homogeneous unbounded media, including full and half-plane wave propagation scenarios. In these cases, Young's modulus is treated as a function of radius, and results are compared with those from the extended mesh method and analytical solutions (where available). The results demonstrate that the VUIR-based SBM significantly reduces computational effort, particularly by reducing cut-off time. For example, choosing a cut-off time of 300 can lead to up to a 91% reduction in computational effort. This makes the VUIR-based SBM a highly efficient tool for solving dynamic wave propagation problems.

Keywords: Scaled boundary method; Velocity; Semi-analytical method; Unbounded domains; Non-homogeneous; Cut-off time.

I. INTRODUCTION

Over the last decades, the classical boundary element method (BEM) was employed to investigate a variety of engineering problems. Seepage (Rafiezadeh & Ataie-Ashtiani, 2012), static (Ribeiro & de-Paiva, 2014), and dynamic (Pak & Guzina, 1999) phenomena were successfully evaluated using the BEM. The BEM demands a fundamental solution in each analysis, which should precisely satisfy the governed equations in the problem domain (Wolf, 2003). Determining a fundamental solution for complicated geometries can be challenging. Since 1996, Wolf & Song (1996) have presented a fundamental solution less BE approach, which later was named the scaled boundary finite element method (SBFEM). This innovative numerical technology has an analytical solution procedure for the entire domain while it solves governing equations numerically on boundaries. Therefore, the SBFEM utilizes the benefits of the two most widely used methods in engineering problems, the finite element method (FEM) and the boundary element method (Deeks & Wolf, 2002). In this procedure, the governing equations should be transformed to the scaled boundary coordinate system. The scaled boundary coordinate system contains a scale center (SC) and two or three dimensionless local coordinates (η, ξ, and ς) for 2D and 3D problems, respectively. Figure 1 depicts the SBM mesh generation scheme.

Like BEM, the SBM has been utilized to solve a broad range of engineering problems over the years. This approach is used to assess seepage (Bazyar & Talebi, 2015), static (Lin et al., 2014), and dynamic problems (Genes & Kocak, 2005; Yaseri et al., 2014). In most previous studies, a homogeneous problem domain has been considered (Hajialilue-Bonab & Tohidvand, 2015). Researchers have developed a dynamic stiffness-based scaled boundary method (SBM) in the frequency domain (Syed & Maheshwari, 2015) and an acceleration unit impulse response (AUIR)-based method in the time domain (Bazyar & Song, 2006a,b) for wave propagation modeling in non-homogeneous infinite media. Advantages of implementing SBM to model unbounded media compared to other approaches, such as perfectly matched layer (PML), infinite element method (IEM), and BEM can be stated as follows:

- In contrast with the BEM, the SBM does not require fundamental solutions. This property makes the SBM more applicable in solving engineering problems.
- The SBM is faster than the BEM regarding computational effort.
- Considering the main drawbacks of the IEM, formulation of the SBM is straightforward similar to the conventional finite element approach and no further

assumption is needed to extract dynamic stiffness of unbounded media.
- While the PML does not reduce the dimension of the problem, the SBM reduces geometrical dimension of problems by one.

Figure 2 shows the diagonal entries of the AUIR matrix (a). As the figure depicts, the AUIR matrix should be calculated from the starting time (t=0) to the end of the analysis (t=T, T is the period of the vibration). Calculating the AUIR matrix (in a global procedure) can be more expensive and saving such a large matrix in the computers may be problematic. Computational efforts of the SBM for determining the response matrix can be reduced by using the velocity unit impulse response (VUIR) matrix instead of the AUIR matrix. Diagonal entries of the velocity unit impulse responses can be considered as Figure 2(b). Referring to the figure, after a truncation time (t_c), VUIR can be considered equal to a constant value. Hence, determining the response matrix may be limited to the time interval [0, t_c].

The scaled boundary equation in VUIR has been derived for homogeneous unbounded media previously, and this response was used to construct the displacement unit impulse response (DUIR) matrix (Wolf, 2003). Calculating interaction force using the DUIR matrix (Eq. 1) may lead to a more complicated formulation (Chen et al., 2014). This formulation can reduce computational efforts of the SBM; however, it also makes understanding the resulting procedure more difficult.

In this paper, VUIR matrices are used directly to determine interaction forces (Eq. 2). In Eqs. 1 and 2, S^{∞} and V^{∞} are DUIR and VUIR matrices, respectively. In these equations, u, u̇, and R are displacement, velocity, and interaction force vectors, respectively.

$$\{R(t)\} = \int_0^t [S^{\infty}(t-\tau)]\{u(\tau)\}\, d\tau \quad (1)$$

$$\{R(t)\} = \int_0^t [V^{\infty}(t-\tau)]\{\dot{u}(\tau)\}\, d\tau \quad (2)$$

Eqs. 1 and 2 can be used for dynamic problems, whereas they should be modified for seismic problems. In this research, only the dynamic condition is considered. To the authors' best knowledge, this is the first time that the velocity-based SBM is used directly for modeling wave propagation problems. At the time of this research, related information regarding the effects of the truncation time of the velocity responses on the accuracy of achieved answers could not be found, thus, it is studied in this paper comprehensively. To compare VUIR with the previously used scaled boundary approaches like the acceleration unit impulse response and displacement unit impulse based methods, following can be considered:
- Derivation of DUIR-based method is more complicated than the acceleration and velocity unit impulse response-based methods; however, DUIR needs less computational effort.
- Using DUIR based SBM in modeling wave propagation problems (where interaction between near and far-field must be considered) leads to more complicated procedures in comparison with the other two methods.

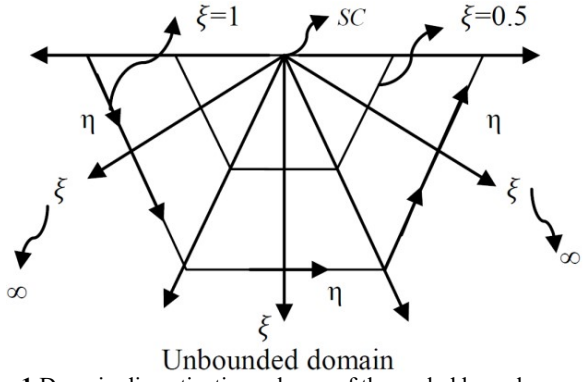

Fig. 1 Domain discretization scheme of the scaled boundary method (Deeks & Wolf, 2002)

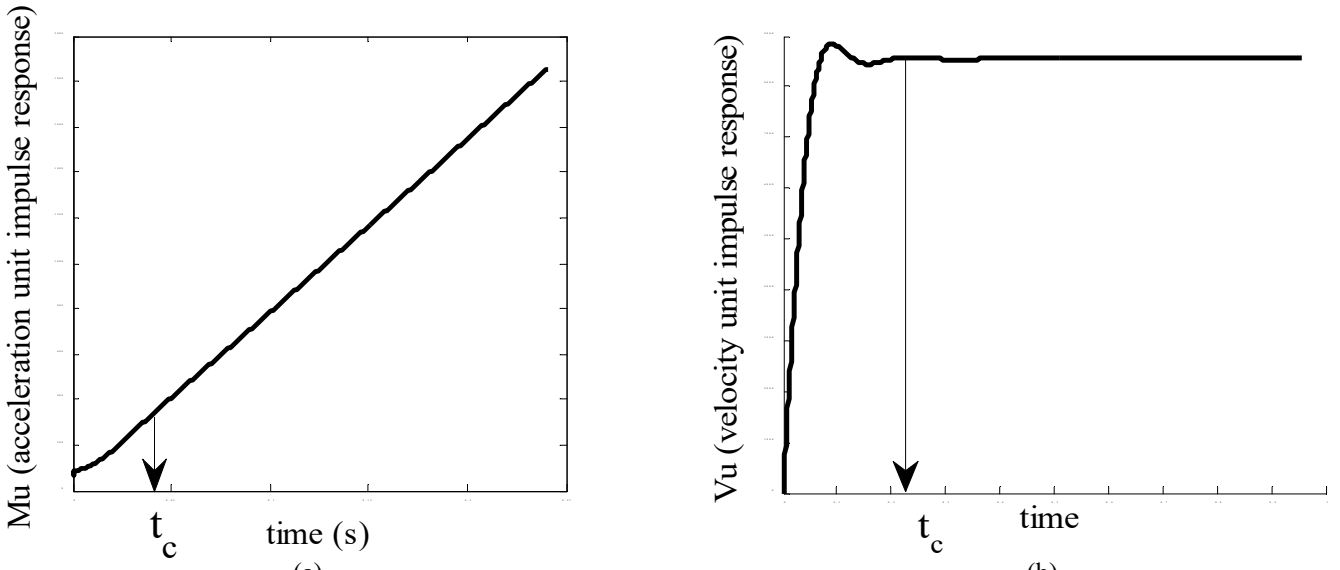

Fig. 2 Diagonal entries of (a) acceleration unit impulse response matrix (b) velocity unit impulse response matrix (Bazyar & Song, 2006b)

- More simplifying assumptions are needed in DUIR based method, and these simplifications induce more approximations in the results.
- VUIR based SBM requires less computational efforts in comparison with the acceleration unit impulse response-based method without any significant reduction in accuracy.

Wolf & Song (1996) proposed the scaled boundary formulation of the displacement unit impulse response matrix for the first time. Chen et al. (2014) presented an enhanced scaled boundary formulation for wave propagation problems in anisotropic soils. Birk et al. (2017) used a displacement unit impulse response based scaled boundary approach for wave propagation in heterogeneous soils.

In this paper, VUIR based scaled boundary method is extended to model non-homogeneous unbounded media. Previous studies (on homogenous media) have used velocity unit impulse matrix to develop displacement unit impulse matrix, while, in this paper, the interaction forces are extracted directly using by VUIR matrix. This eliminates complicated formulations required in the DUIR based scaled boundary method and the large time consumption of AUIR based method. The paper is structured with providing a short review of SBM, deriving the modified scaled boundary equation for VUIR matrix, presenting its implementation steps, and evaluating its precision and reliability, and solving few benchmarks numerical examples. However, the proposed method has various advantages including less computation effort, and higher accuracy, there are some limitations for the presented novel method. These limitations can be stated as follows:

- The proposed method is valid only for elastic far field.
- The proposed method is valid only for dry soil media.
- This method can only be considered for modeling of far fields, where another numerical approach should be coupled with it to simulate near field effects.

II. Materials and Methods

A. Principal of SBFEM

To model wave propagation in unbounded media, various numerical approaches have been used in the literature. The conventional FEM requires discretizing entire problem domain and is not capable of modeling unbounded domains. Wave propagation problems can be solved using the FEM by adopting large elements extended to an adequate distance from problem domain to ensure reflected wave from the boundaries have insignificant effect on the domain. This approach is called extended mesh method (EMM). Due to the computational costs incurred using the EMM; it is impractical to use it without considering absorbing boundaries. In contrast to the FEM, the BEM discretizes only boundaries of the problem and reduces dimension of the problem by one. The BEM is capable of modeling unbounded media using fundamental solutions with a semi-analytical approach. Extraction of a fundamental solution for different problems can be complicated, and it makes application of the BEM for practical problems more difficult. In addition, numerical difficulties such as integral singularities may occur using the BEM.

The SBM is a semi-analytical approach that can be employed to accurately simulate finite and infinite media (Hassanzadeh et al., 2018). To understand the proposed extended method provided herein, it is deemed necessary to review basic equations SBM in the following which E_0, E_1, E_2, and M_0 are four coefficient matrices of the SBM, calculated using Eq. 3 to 6, respectively (Deeks & Wolf, 2002) as follow.

$$[E^0]=\int_{-1}^{+1}[B^1]^T[D][B^1]\,|J|\,d\eta \tag{3}$$

$$[E^1]=\int_{-1}^{+1}[B^2]^T[D][B^1]\,|J|\,d\eta \tag{4}$$

$$[E^2]=\int_{-1}^{+1}[B^2]^T[D][B^2]\,|J|\,d\eta \tag{5}$$

$$[M^0]=\int_{-1}^{1}[N(\eta)]^T\rho[N(\eta)]\,|J|d\eta \tag{6}$$

where [D] indicates the elasticity matrix, [ρ] is used for density matrix, and $[B^1]$ and $[B^2]$ are matrices that contain shape functions and derivatives of shape functions (Wolf, 2003). A unit impulse response must be computed for time-domain modeling of wave propagation in unbounded domains using the SBM. For homogeneous infinite media, scaled boundary equations for these responses have been derived. Wolf (2003) presented the scaled boundary equation in dynamic stiffness for frequency domain analysis of non-homogeneous infinite media (Eq. 7). In Eq. 7, α and β are non-homogeneity parameters of elasticity and density, respectively, and s is the parameter of dimension (s=2 for 2D and s=3 for 3D problems). In this equation, material properties are used as a power function of the radial coordinate (ξ).

$$\begin{aligned}&([S^\infty(\omega)]+[E^1])[E^0]^{-1}([S^\infty(\omega)]+[E^1]^T)\\&-(s-2)[S^\infty(\omega)]-\omega[S^\infty(\omega)]_{,\omega}\\&-[E^2]+\omega^2[M^0]=0\end{aligned} \tag{7}$$

Bazyar & Song (2006a) improved the SBM for spatially non-homogeneous materials. They used Eqs. 8 and 9 to calculate the elastic modulus and mass density in their research (for 2D problems).

$$E(x,y)=\xi^\alpha E(\eta)=\xi^\alpha\left(\sum_{i=1}^{2}m_{Ex_i}\left(\frac{|x_i(\eta)|}{L}\right)^\alpha+m_{Er}\left(\frac{|r(\eta)|}{L}\right)^\alpha\right) \tag{8}$$

$$\rho(x,y)=\xi^\beta\rho(\eta)=\xi^\beta\left(\sum_{i=1}^{2}\rho_{x_i}\left(\frac{|x_i(\eta)|}{L}\right)^\beta+\rho_r\left(\frac{|r(\eta)|}{L}\right)^\beta\right) \tag{9}$$

where m_{Exi} and ρ_{xi} are constants with the units of elastic modulus and mass density that are used to scale the material properties in these equations. Only the scaled boundary equation in AUIR has been developed for time-domain analysis of non-homogeneous unbounded media. Eq. 10 was derived by Bazyar & Song (2006b) to establish AUIR for non-homogeneous unbounded media.

$$\int_0^t [M^\infty(t-\tau)][E^0]^{-1}[M^\infty(\tau)]d\tau + (1-0.5\alpha+.5\beta)t\int_0^t [M^\infty(\tau)]d\tau +$$
$$([E^1][E^0]^{-1} - (0.5(s+1)-0.25\alpha+0.75\beta)[I])\int_0^t\int_0^\tau [M^\infty(\tau')]d\tau' d\tau +$$
$$\int_0^t\int_0^\tau [M^\infty(\tau')]d\tau' d\tau([E^0]^{-1}[E^1]^T - (0.5(s+1)-0.25\alpha+0.75\beta)[I]) - \quad (10)$$
$$\frac{t^3}{6}([E^2]-[E^1][E^0]^{-1}[E^1]^T)H(t) - t[M^0]H(t) = 0$$

In Eq. 10, the $H^{(t)}$ indicates the Heaviside-step function. It is worth mentioning that, for non-homogeneous unbounded media, the essential coefficient matrices (Eqs. 3 to 6) should be calculated by the modified equations. The modified equations are detailed in Eqs. 11 to 14.

$$[E^0] = \int_{-1}^{+1} [B^1]^T [D(\eta)][B^1] \mid J \mid d\eta \quad (11)$$

$$[E^1] = \int_{-1}^{+1} [B^2]^T [D(\eta)][B^1] \mid J \mid d\eta \quad (12)$$

$$[E^2] = \int_{-1}^{+1} [B^2]^T [D(\eta)][B^2] \mid J \mid d\eta \quad (13)$$

$$[M^0] = \int_{-1}^{1} [N(\eta)]^T \rho(\eta)[N(\eta)] \left|J\right| d\eta \quad (14)$$

Since the unit impulse response of infinite media is calculated, interaction forces can be determined (Eq. 1 and 2). DUIR matrix can be stated as follows (Wolf, 2003; Rahnema et al., 2016; Aslmand et al., 2019):

$$S^\infty(t) = C_\infty \dot{\delta}(t) + K_\infty \delta(t) + S_r(t) \quad (15)$$

In Eq. 15, C^∞, K^∞, and δ(t) are constant damping matrix of unbounded media, constant stiffness matrix of unbounded media, and the Dirac delta function, respectively. Sr∞ is the regular portion of the DUIR matrix. The required formulation for C^∞ and K^∞ (for both homogeneous and non-homogeneous cases) was derived previously (Wolf, 2003). Substituting Eq. 15 within Eq. 1 yields the new form of the interaction force as follow:

$$\{R(t)\} = C_\infty \dot{u}(t) + K_\infty u(t) + \int_0^t [S_r^\infty(t-\tau)]\{u(\tau)\} d\tau \quad (16)$$

Since, integrating displacements can be difficult, the velocity-based responses may be used; hence, interaction force can be considered as Eq. 17 in the frequency domain:

$$R(\omega) = V^\infty(\omega)\dot{u}(\omega) = i\omega V^\infty(\omega) u(\omega) \quad (17)$$

$$S^\infty(\omega) = i\omega C_\infty + K_\infty + S_r(\omega) \quad (18)$$

$$V^\infty(\omega) = \frac{S^\infty(\omega)}{i\omega} \quad (19)$$

By substituting Eqs. 18 and 19 within Eq. 16, in frequency and time domains, the interaction force-velocity relationship can be obtained by performing an inverse Fourier transformation:

$$R(\omega) = C_\infty \dot{u}(\omega) + \frac{K_\infty \dot{u}(\omega)}{i\omega} + \frac{S_r^\infty(\omega)\dot{u}(\omega)}{i\omega}$$
$$= C_\infty \dot{u}(\omega) + K_\infty u(\omega) + V_r^\infty(\omega)\dot{u}(\omega) \quad (20)$$

$$\{R(t)\} = C_\infty \dot{u}(t) + K_\infty u(t) + \int_0^t [V_r^\infty(t-\tau)]\{\dot{u}(\tau)\} d\tau \quad (21)$$

In Eq. 21, V_r^∞ is the regular portion of the VUIR matrix. The scaled boundary equation of VUIR is developed in the following section for non-homogeneous un-bounded media and time discretization of Eq. 21 is presented.

B. Modified formulation forSBFEM

To determine the regular portion of the DUIR matrix, Eq. 18 is substituted into Eq. 7. For simplicity, the coefficient matrices are transformed to the new form, and it is yields into:

$$[e^0] = [\Phi]^T [E^0][\Phi] \quad (22)$$

$$[e^1] = [\Phi]^T [E^1][\Phi] \quad (23)$$

$$[e^2] = [\Phi]^T \quad (24)$$

$$[E^2][\Phi] = [\Phi]\ [M^0][\Phi] \quad (25)$$

$$[c_\infty^0] = [\Phi]^T [C_\infty][\Phi] \quad (26)$$

$$[k_\infty] = [\Phi]^T [K_\infty][\Phi] \quad (27)$$

These equations, Φ is calculated by the Cholesky decomposition of the $[E_0]^{-1}$ as per Eq. 28.

$$[E^0]^{-1} = [\Phi]\,[\Phi]^T \quad (28)$$

The resulted equation for the regular portion of the DUIR matrix is formed in Eq. 29.

$$[s^\infty{}_r]^2 + i\omega([s^\infty{}_r][c_\infty] + [c_\infty][s^\infty{}_r]) + ([e^1] + [k_\infty])[s^\infty{}_r] +$$
$$[s^\infty{}_r]([e^1]^T + [k_\infty]) + ([e^1]^T + [k_\infty])([e^1] + [k_\infty]) - [e^2] - \quad (29)$$
$$(\alpha + s - 2)[s^\infty{}_r] - (\alpha + s - 2)[k_\infty] - (1 - 0.5\alpha + 0.5\beta)\omega[s^\infty{}_r]_{,\omega} = 0$$

By dividing Eq. 29 by $(i\omega)^2$ and substituting Eq. 19, Eq. 30 is derived.

An inverse Fourier transformation can be used to obtain the SBFE equation for the regular portion of the VUIR matrix in the time domain. The resulted formula is shown in Eq. 31. Also, Eq. 31 can be considered as an initial value problem and the initial condition must be selected as Eq. 32 (Wolf, 2003).

$$[v^{\infty}{}_r]^2+[v^{\infty}{}_r][c_\infty]+[c_\infty][v^{\infty}{}_r]+([e^1]+[k_\infty])\frac{[v^{\infty}{}_r]}{i\omega}+$$
$$\frac{[v^{\infty}{}_r]}{i\omega}([e^1]^T+[k_\infty])+\frac{1}{(i\omega)^2}([e^1]^T+[k_\infty])([e^1]+[k_\infty])-$$
$$\frac{[e^2]}{(i\omega)^2}+(1-s-0.5\alpha-0.5\beta)\frac{[v^{\infty}{}_r]}{i\omega}-$$
$$(\alpha+s-2)\frac{[k_\infty]}{(i\omega)^2}-(1-0.5\alpha+0.5\beta)\omega\,[v^{\infty}{}_r]_{,i\omega}=0 \quad (30)$$

$$\int_0^t v^{\infty}{}_r(t-\tau)v^{\infty}{}_r(\tau)d\tau+[v^{\infty}{}_r(t)][c_\infty]+[c_\infty][v^{\infty}{}_r(t)]+$$
$$([e^1]+[k_\infty])\int_0^t[v^{\infty}{}_r(\tau)]d\tau+\int_0^t[v^{\infty}{}_r(\tau)]d\tau([e^1]^T+[k_\infty])+$$
$$t(([e^1]^T+[k_\infty])([e^1]+[k_\infty])-[e^2]-(\alpha+s-2)[k_\infty]) \quad (31)$$
$$+(1-s-0.5\alpha-0.5\beta)\int_0^t[v^{\infty}{}_r(\tau)]d\tau-$$
$$+(1-0.5\alpha+0.5\beta)t[v^{\infty}{}_r(t)]=0$$
$$[v^{\infty}{}_r(t=0)]=[0] \quad (32)$$

It is presumed that the VUIR is piecewise constant over time intervals. By time discretizing Eq. 31, a Lyapunov equation for each time step (t=ndt) can be derived. This linear equation can be written as:

$$(\frac{1}{dt}c_\infty+0.5(([e^1]+[k_\infty])+0.5(1-s-0.5\alpha-0.5\beta+$$
$$n(1-0.5\alpha+0.5\beta))[I]))[v^{\infty}{}_r]_n+[v^{\infty}{}_r]_n(\frac{1}{dt}c_\infty+$$
$$0.5(([e^1]+[k_\infty])+0.5(1-s-0.5\alpha-0.5\beta+$$
$$n(1-0.5\alpha+0.5\beta))[I]))=-\sum_{j=1}^{n-1}[v^{\infty}{}_r]_j[v^{\infty}{}_r]_{n-j}- \quad (33)$$
$$(([e^1]+[k_\infty])+0.5(1-s-0.5\alpha-0.5\beta)[I])\sum_{j=1}^{n-1}[v^{\infty}{}_r]_j-$$
$$\sum_{j=1}^{n-1}[v^{\infty}{}_r]_j(([e^1]+[k_\infty])+0.5(1-s-0.5\alpha-0.5\beta)[I])+$$
$$n([e^2]+(s+\alpha-2)[k_\infty]-([e^1]+[k_\infty])([e^1]^T+[k_\infty]))$$

The original form of the VUIR matrix must be calculated by:

$$[V^{\infty}{}_r]_n=[\Phi]^{-T}[v^{\infty}{}_r]_n[\Phi]^{-1} \quad (34)$$

After calculating the response matrix, by using Eq. 21, interaction force for dynamic cases can be achieved. By time discretizing this equation and by using the Newmark time integrating method (Wolf, 2003), Eq. 35 can be formed.

$$\{R\}_n=[C_\infty]\{\dot u\}_n+[K_\infty]\{u\}_n+\sum_{j=1}^{n}[V^{\infty}{}_r]_{n-j+1}(\{u\}_j-\{u\}_{j-1})$$
$$[C_\infty]\{\dot u\}_n+[K_\infty]\{u\}_n+\beta_1dt^2[V^{\infty}{}_r]_1\{\ddot u\}_n+dt[V^{\infty}{}_r]_1\{\dot u\}_{n-1}+$$
$$(0.5-\beta_1)dt^2[V^{\infty}{}_r]_1\{\ddot u\}_{n-1}+\sum_{j=1}^{n-1}[V^{\infty}{}_r]_{n-j+1}(\{u\}_j-\{u\}_{j-1})= \quad (35)$$
$$[C_\infty]\{\dot u\}_n+[K_\infty]\{u\}_n+\beta_1dt^2[V^{\infty}{}_r]_1\{\ddot u\}_n+\{F_\Gamma\}_n$$

Where β_1 is the constant parameter of the Newmark method. In the use of Eq. 35, $[V_r^{\infty}]$ can be calculated up to the truncation time (t_c) then it can be selected equal to the constant value $[V_r^{\infty}(t=t_c)]$. Based on the substructure method, the equation of motion can be stated as:

$$\begin{bmatrix}K_{ii} & K_{i\Gamma}\\ K_{\Gamma i} & K_{\Gamma\Gamma}+K_\infty\end{bmatrix}\begin{bmatrix}u_i(t)\\ u_\Gamma(t)\end{bmatrix}+\begin{bmatrix}C_{ii} & C_{i\Gamma}\\ C_{\Gamma i} & C_{\Gamma\Gamma}+C_\infty\end{bmatrix}\begin{bmatrix}\dot u_i(t)\\ \dot u_\Gamma(t)\end{bmatrix}+$$
$$\begin{bmatrix}M_{ii} & M_{i\Gamma}\\ M_{\Gamma i} & M_{\Gamma\Gamma}+\beta_1dt^2[V^{\infty}{}_r]_1\end{bmatrix}\begin{bmatrix}\ddot u_i(t)\\ \ddot u_\Gamma(t)\end{bmatrix}=\begin{bmatrix}p_i(t)\\ p_\Gamma(t)-\{F_\Gamma\}_n\end{bmatrix} \quad (36)$$

In Eq. 36, the subscript (Γ) represents degrees of freedom on the near and far-field border and the subscript (i) is used for remaining degrees of freedom (DOFs) which is presented in Figure 3.

C. Method Implementation

The flowchart of the implementation method is shown in Figure 4. As this figure shows, the computation process involves three different stages including preprocessing, where all of the required information will be introduce to the code, processing, where the calculation will be undertaken, and post processing, where all of the required plots will be prepared. All of the process will be adapted using self written MATLAB codes.

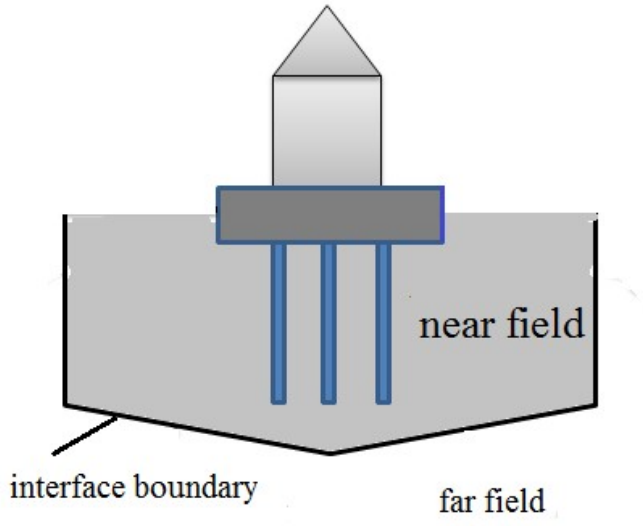

Fig. 3 Domain discretization scheme in the sub-structure method (Bazyar & Song, 2006b)

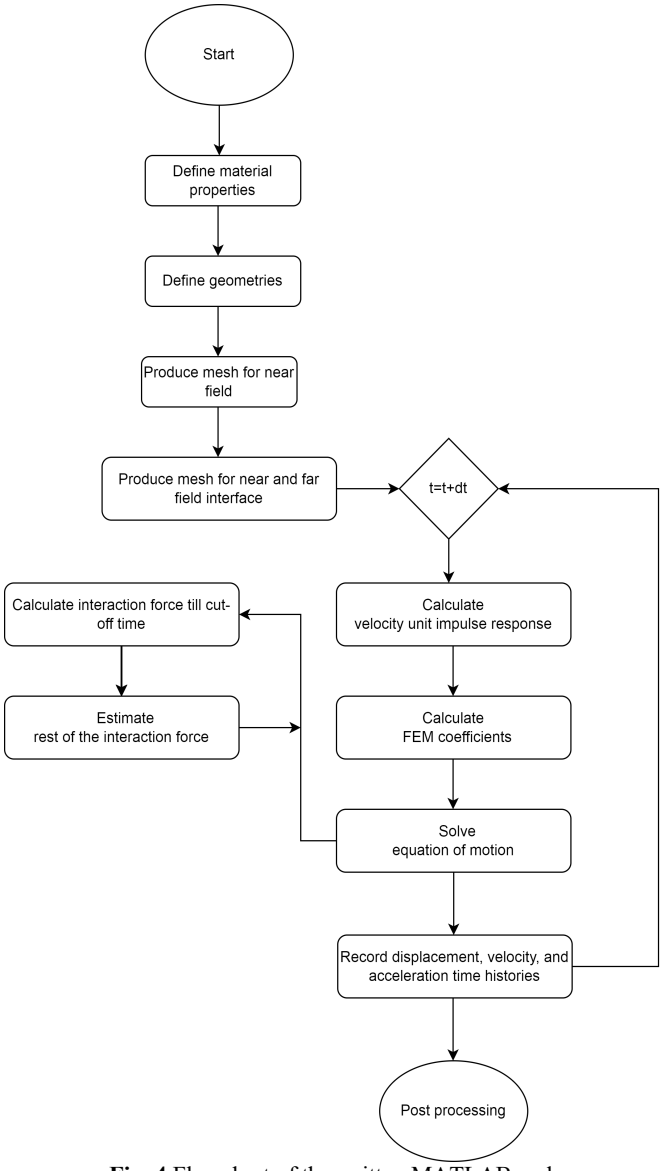

Fig. 4 Flowchart of the written MATLAB code

III. Results and Discussion

Several numerical examples are solved to examine performance of the suggested modified SBM. Three examples are presented to assess the method's precision in modeling wave propagation in both homogeneous and non-homogeneous infinite media. The impact of the truncation time on the results is later assessed.

A. A Full Plane with a Circular Cavity

This example is designed to investigate the accuracy of the presented method for wave propagation modeling in infinite media with non-homogeneity in the radial direction. A circular cavity with a radius of 2 m, embedded in an elastic full plane is considered. The wall of the cavity is subjected to uniform pressure. Based on the substructure method, a small portion of the full plane is modeled by the FEM while modeling of the unbounded media is undertaken by the SBM. Two models are used in the FEM-SBM analyses where model B uses more DOFs in comparison with model A. The considered geometry and used meshes for this example are presented in Figure 5(a) and Figure 5(b). As this figure shows, by using symmetry, only one-quarter of the problem is examined. A triangular function which is defined in Figure 6(a) is used to describe the time history of the applied uniform pressure. The applied load has a period of 0.1 seconds and a peak value of 10kN. The EMM is carried out to verify used FEM-SBM approach (EMM is a conventional method for modeling unbounded domain (Bazyar & Song, 2006a).

In the EMM, 1375 nodes (2750 DOFs) are used. Figure 6(b) shows the used extended mesh for this problem. There is an analytical solution for this problem in the literature, for example can be found in Bazyar & Song (2006b). For homogeneous cases (α and β equal to zero), the analytical solution can be compared with both the extended mesh procedure and the scaled boundary approach. For homogeneous case, material properties are considered as elasticity modulus (E), E=18720 kN/m^2, Poisson's ratio, v=0.3, and mass density, ρ=2×103 kg/m^3. Achieved radial displacement time histories for the cavity wall are plotted in Figure 7. It is shown that both velocity unit impulse response-based scaled boundary models lead to good agreement with the EMM and with the analytical solution (maximum error of the proposed SBM is equal to 10%). In the EMM, 1375 nodes (2750 DOFs) are used. Figure 6(b) shows the used extended mesh for this problem. For homogeneous cases (α and β equal to ZERO), the analytical solution can be compared with both the extended mesh procedure and the scaled boundary approach. For homogeneous case, material properties are considered as E=18720 kN/m^2, v=0.3, and ρ=2×103 kg/m^3. Achieved radial displacement time histories for the cavity wall are plotted in Figure 7. It is shown that both velocity unit impulse response-based scaled boundary models lead to good agreement with the EMM and with the analytical solution (maximum error of the proposed SBM is equal to 10%).

For non-homogeneous cases, E of the full plane is considered as a function of radius, which is introduced by the last term in Eq. 8. The characteristic length (L) is selected equal to three. The scaling value of the elasticity modulus (m_{Er}) is selected equal to m_{Er}=18720 kN/m^2. Other mechanical properties are considered constant with the values of v=0.3 and ρ=2×103 kg/m^3. Figure 8 shows the variation of elastic modulus in the radial direction with considering α equal to one for the mesh that is used in the EMM.

Three different situations are regarded to analyze the precision of the proposed SBM in non-homogeneous media. Obtained radial displacement time histories of the cavity wall are plotted in Figure 9. Figure 9 demonstrates a good agreement between the VUIR-based SBM and the EMM.

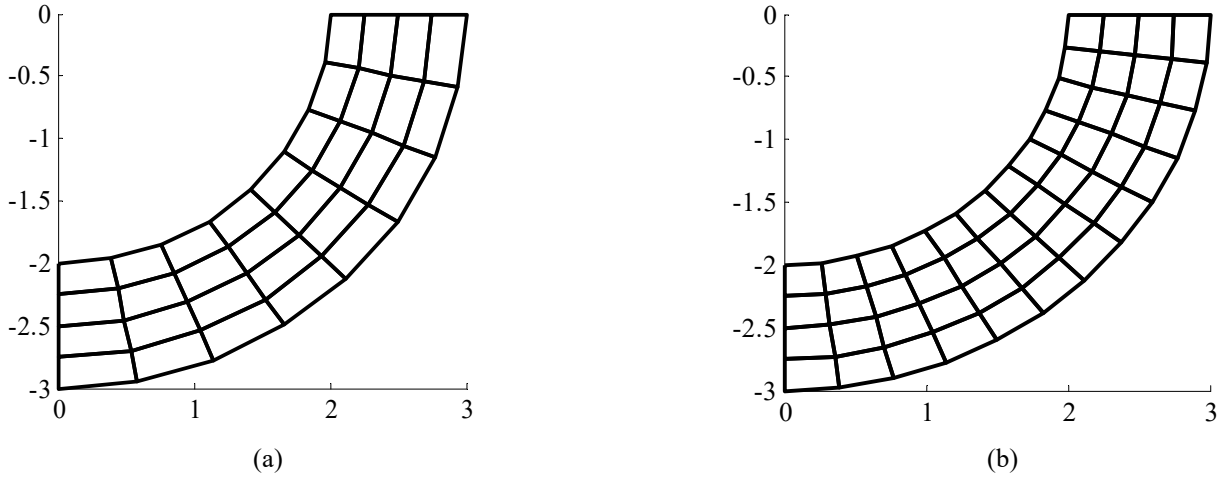

Fig. 5 Used models for modeling circular cavity in full plane: (a) Model A (DOFs=90) (b) Model B (DOFs=130)

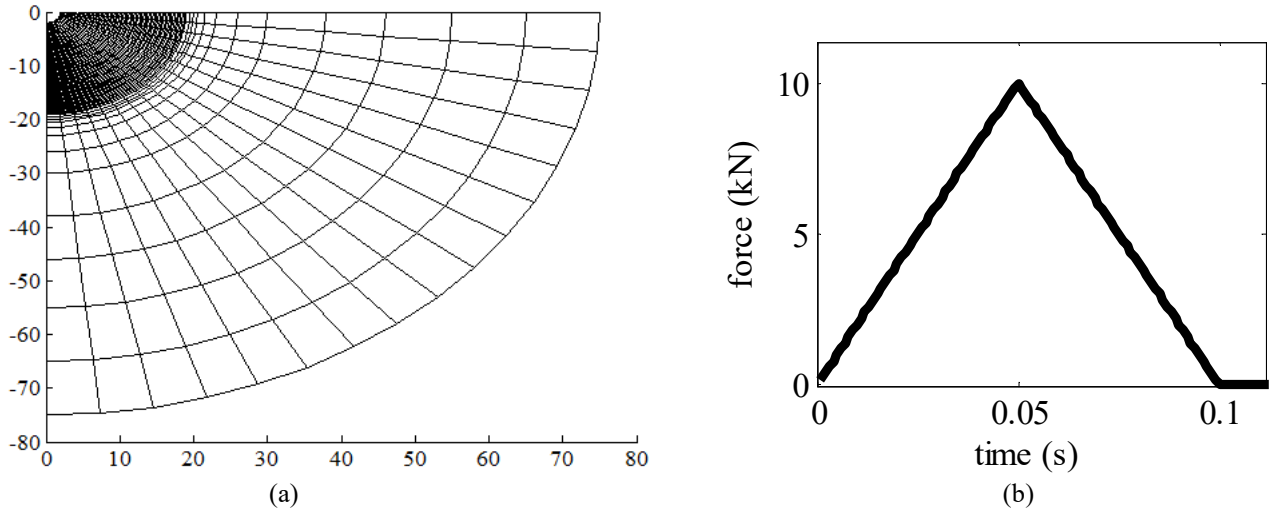

Fig. 6 Modeling a circular cavity embedded in full plane: (a) Time history of the pressure (b) Extended mesh

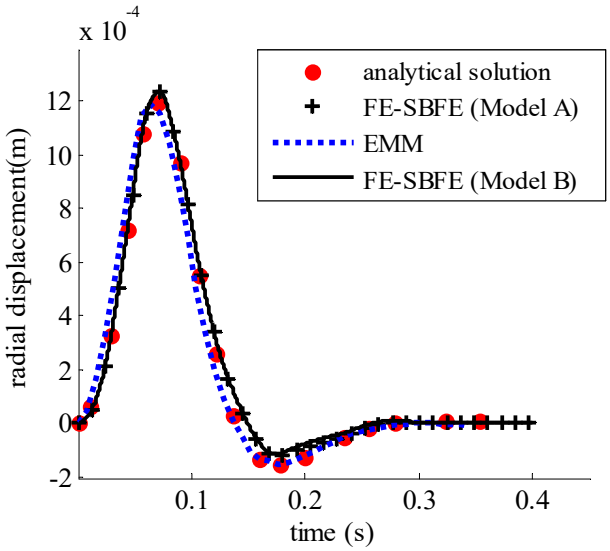

Fig. 7 Radial displacement time history of cavity wall (homogenous case)

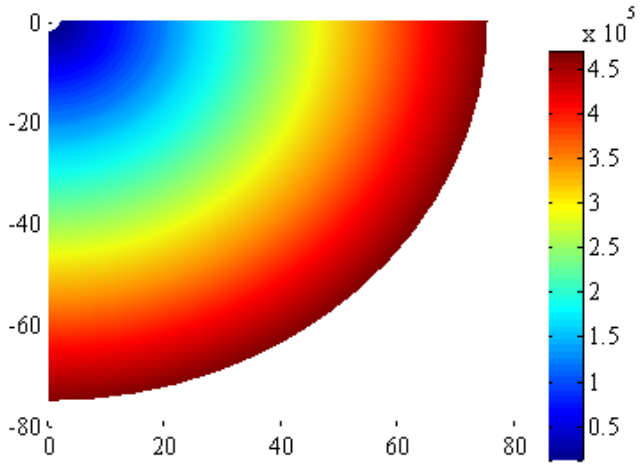

Fig. 8 Variation of elastic modulus in extended mesh

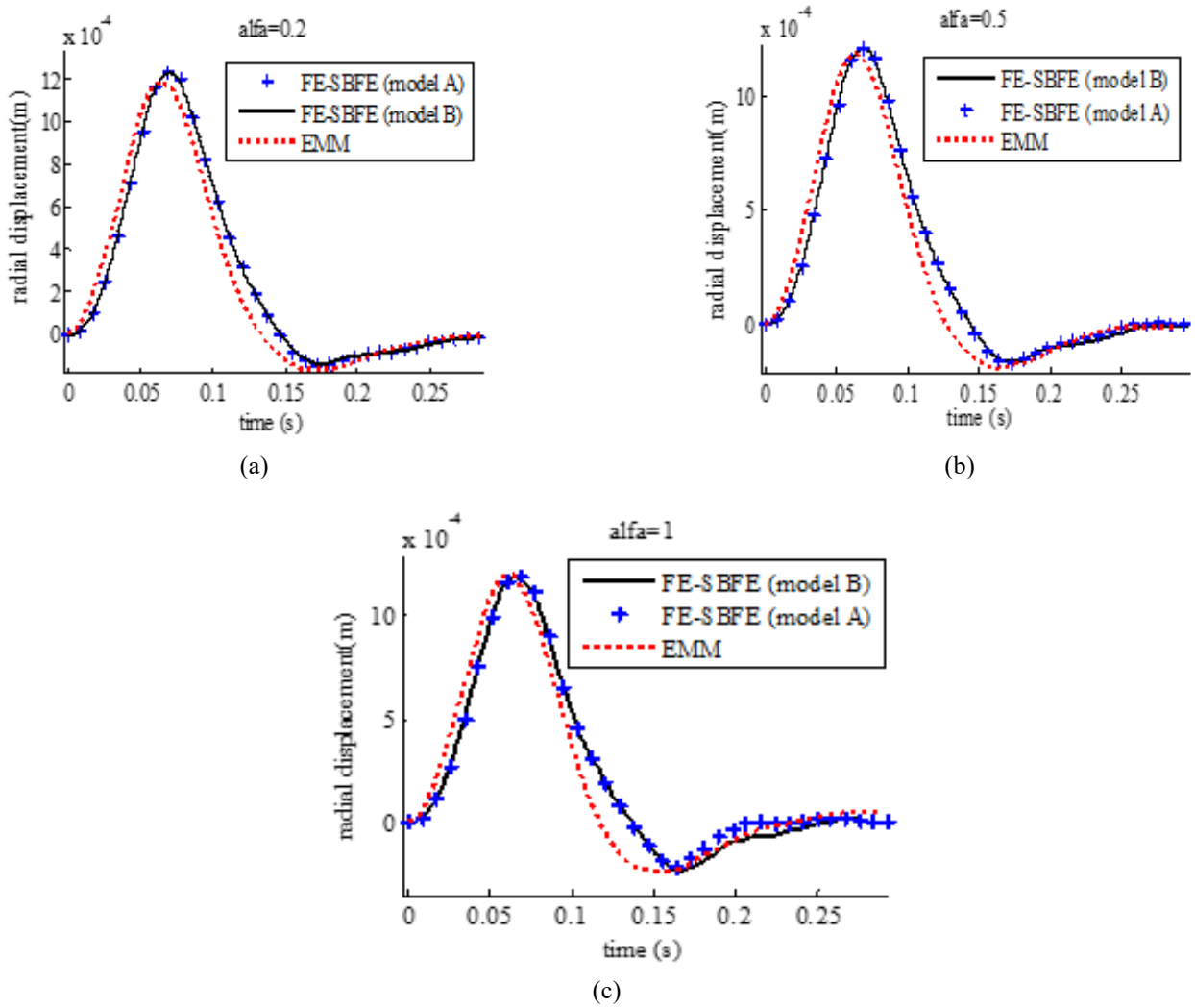

Fig. 9 Radial displacement time history of cavity wall embedded in non-homogenous full plane (a) α=0.2 (b) α=0.5 (c) α=1

B. Horizontal Dynamic Load Applied to an Elastic Half-Plane

An elastic half-plane, as illustrated in Figure 10(a), is used to evaluate the effectiveness of the proposed method in modeling wave propagation in unbounded domains with non-homogeneity in depth. A Ricker wavelet type horizontal dynamic load function is applied to the half-plane under consideration. The material properties in this example are, the scaling elasticity modulus of half-plane, m_{Ez}=2.66×105 kN/m^2, v=0.33 and ρ=2×103 kg/m^3. The dynamic load is applied at point B which provided within Figure 10(a) where the used load function is shown in Figure 10(b). An extended mesh is generated for this problem with height and width equal to 1400m and 6200m, respectively. Figure 11 presents the used FEM-SBM mesh and the extended mesh for this problem.

In the FEM-SBM method, 81 nodes are used while 1125 nodes are employed in the EMM. Firstly, the homogeneous case (α=0 and β=0) is considered. Von Estorff & Firuziaan (2000) used the coupled FEM-BEM to analyze this problem (in homogeneous condition), and their results are used to verify the VUIR based FEM-SBM method and the EMM for homogeneous cases in this paper. The mentioned procedures are used to compute the displacement time histories of point A. Figure 12 show the responses that were obtained. As shown in this figure, the findings are in conformance, indicating that the EMM and the modified scaled boundary method can be used to accurately model this problem. By increasing the period of the vibration, reflected waves can affect the accuracy of the answer in the EMM while the FEM-SBM can be used for any considered period without any wave reflections.

To analyze wave propagation in the non-homogeneous half-plane, the characteristic length is selected equal to 70m. Three cases with α=0.2, α=0.5, and α=1 are considered (for all cases β=0). Other mechanical properties are selected identical to the homogeneous case. Non-homogeneity is assigned only to the depth of the domain. As an example, the variation of the elastic modulus for α=1 in the extended mesh is plotted in Figure 13. Calculated horizontal displacement time histories at the point A are presented in Figure 14. To avoid the effects of the reflected waves in the EMM, only 2.5 seconds of the vibrations are plotted. The EMM and FEM-SBM results demonstrate conformance, as seen in the Figure 14. Hence, it can be concluded that the presented VUIR based SBM has sufficient accuracy for modeling wave propagation in both homogeneous and non-homogeneous unbounded domains.

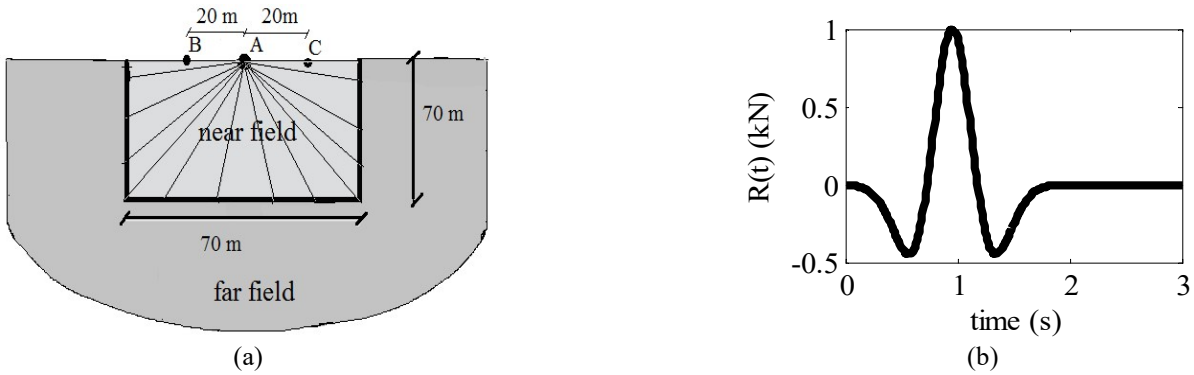

(a) (b)

Fig. 10 (a) Geometry of the problem (half plane) (b) Time history of the load function

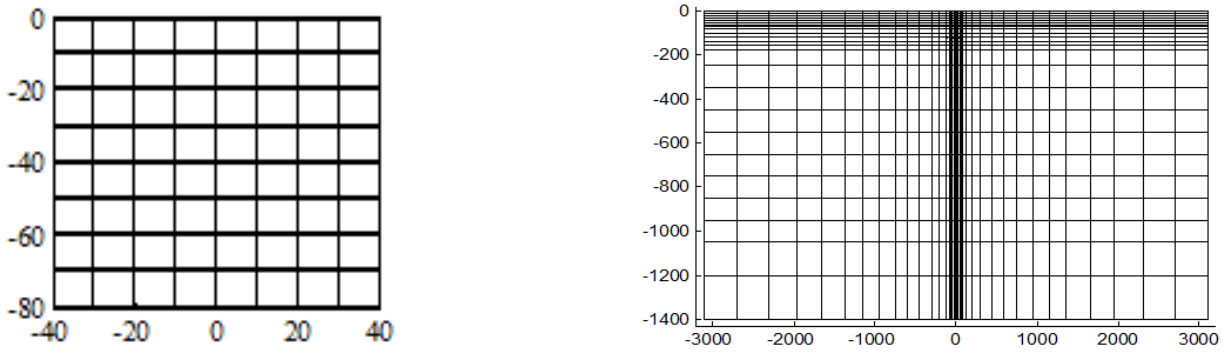

(a) (b)

Fig. 11 Used meshes for (a) FEM-SBM analysis (b) extended mesh method

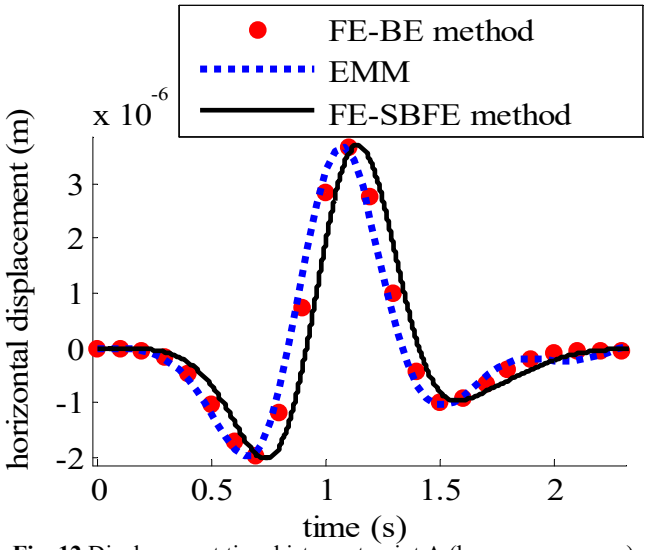

Fig. 12 Displacement time history at point A (homogenous case)

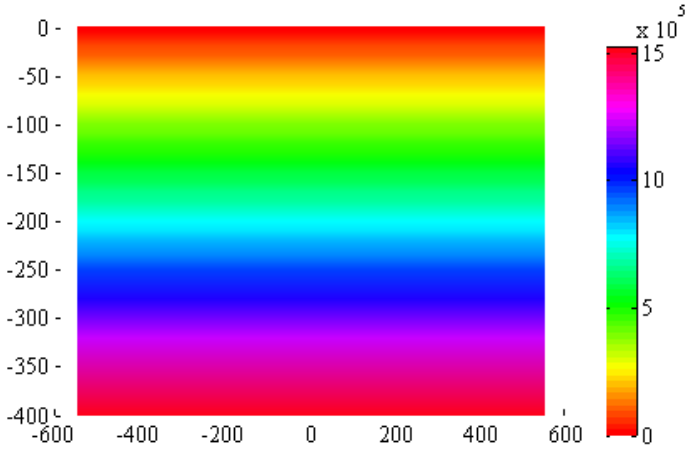

Fig. 13 Variation of elastic modulus with depth in extended mesh

C. A Vertical Dynamic Load Applied to an Elastic Half-Plane

To ensure that the presented method performs well in different loading conditions, another example is solved. This example was used by researchers to verify various numerical approaches. In this paper, results that were published by Von Estorff & Firuziaan (2000) are extracted for homogeneous cases. The geometry of the problem, load function, and generated mesh are detailed in Figure 15. Mechanical properties for the domain are, the elasticity modulus (E) set to E=1.77107 kN/m^2, the Poisson's ratio set to 0.25, and the shear wave velocity set to 474 m/s. Figure 16 shows the displacement time histories of points A, B, and C. The outcome of the three different techniques is depicted in this figure. Results of the FEM-BEM are derived from literature and compared to the extended mesh and the proposed velocity unit impulse response-based methods. The results show good agreements between the applied methods. Maximum deviation between results of the FEM-BEM and the proposed FEM-SBM is 7%. In the next example, the effects of the truncation time on the accuracy of the method, run time of the analyses, and computational efforts are investigated.

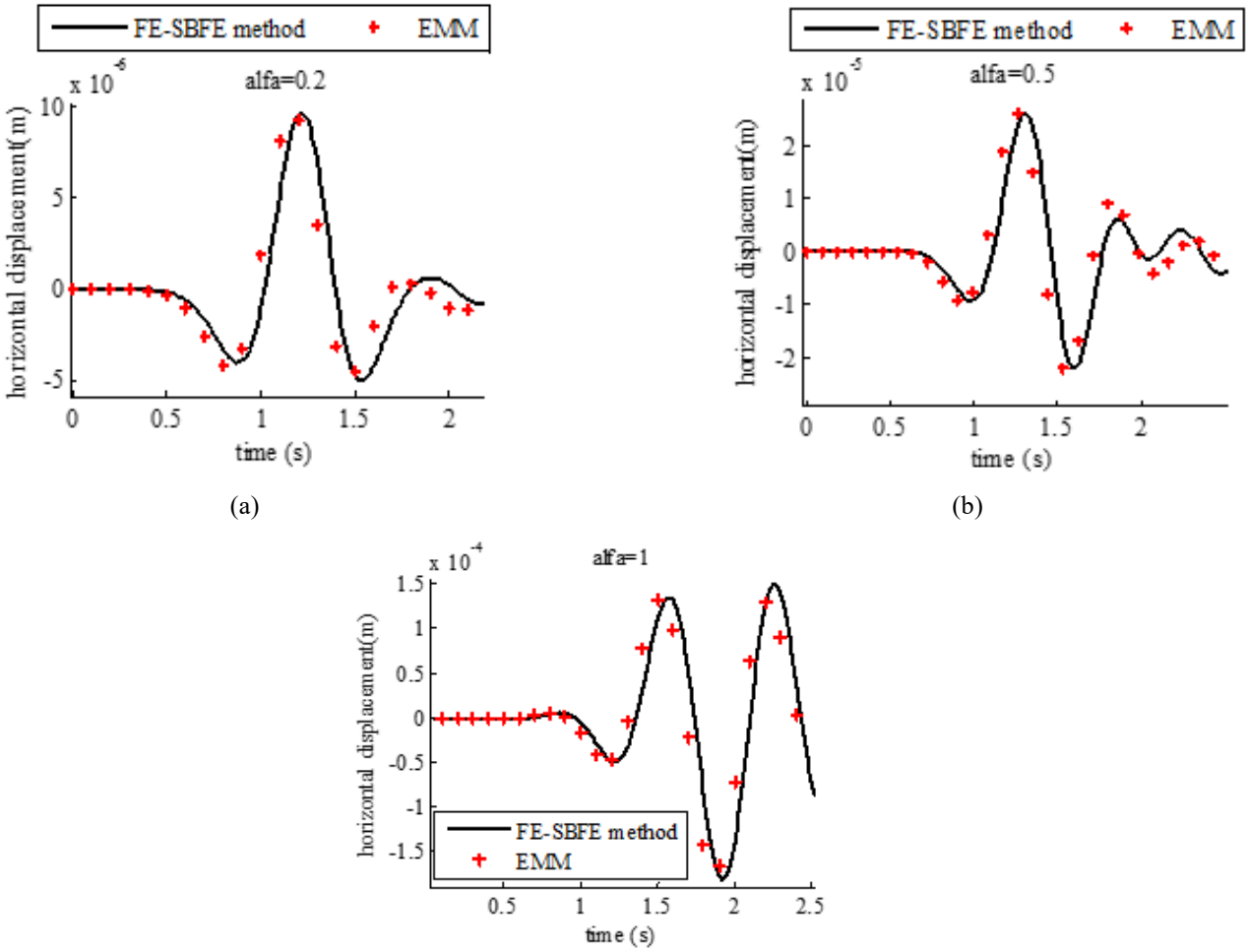

(a) (b) (c)

Fig. 14 Displacement time history at point A in non-homogenous half plane (a) α=0.2 (b) α=0.5 (c) α=1

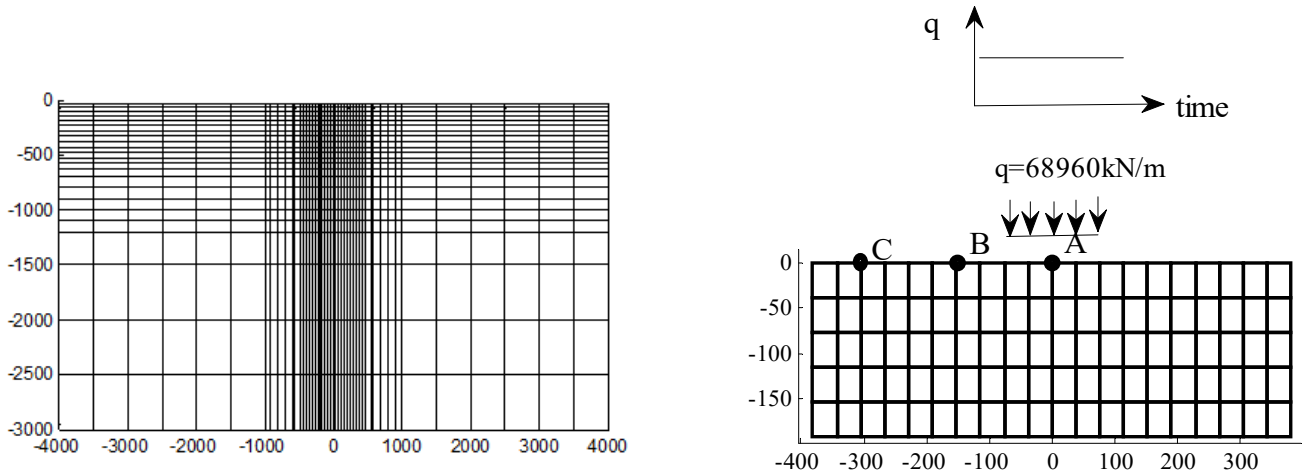

(a) (b)

Fig. 15 Used meshes for (a) extended mesh method (b) FEM-SBM analysis

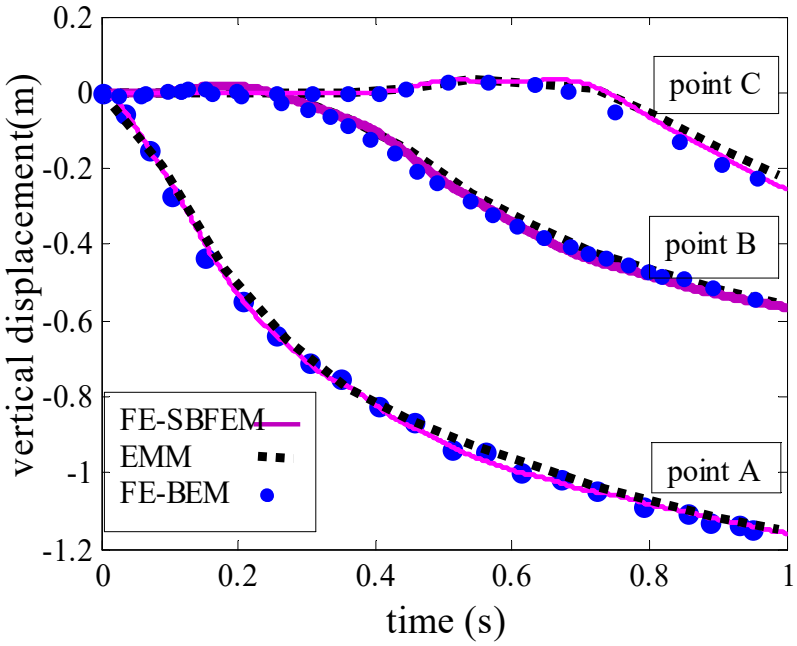

Fig. 16 Displacement time histories for three observation points

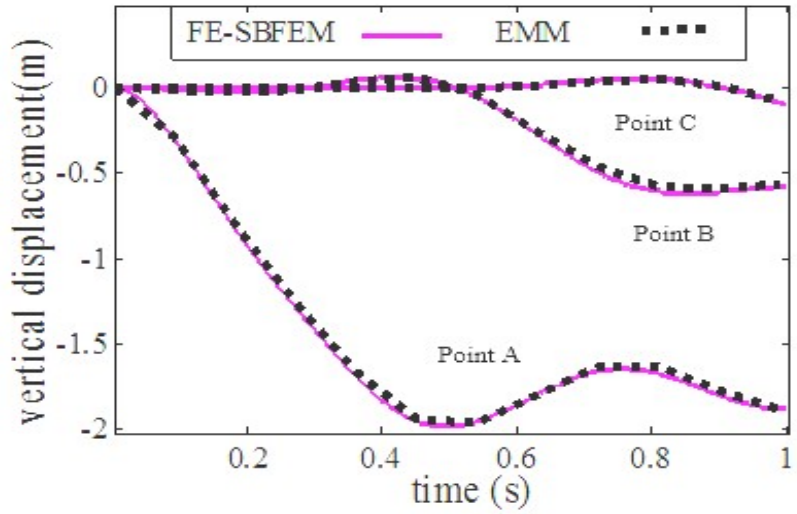

Fig. 17 Displacement time histories of three observation points (non-homogenous case, α=0.5)

D. Soil-Structure Interaction Problem

To assess the effects of the selected truncation time on the accuracy of the answers, a dynamic soil-structure interaction (SSI) problem is considered. In this example, an elastic block attached to an elastic half-plane is examined. The problem's geometry is shown in Figure 18. This figure also shows the mesh that was used and the location of the observation point (point B). Mechanical properties of the block, bounded soil media, and modeled half-plane are selected as E=2.66×105 kN/m^2, v=0.33, and ρ=2×103 kg/m^3. Yazdchi et al. (1999) solved this example previously using the FEM-BEM and their results are used herein to verify the VUIR based SBM. The applied force is chosen as a step function. Duration of the step load function is selected equal to 0.0225s with unit intensity. The conventional FEM-SBM is used to validate the accuracy of the method. The horizontal displacement of point B is plotted in Figure 19(a), which is caused by the horizontal loading (see Figure 18), and the vertical displacement of this point (caused by the vertical loading) is shown in Figure 19(b). Good agreements can be found between the used methods in these figures.

To investigate effects of the selected truncation time on the accuracy of the answers, three different truncation times (t_c) are selected. Figure 20 shows the obtained results for the vertical displacement time history of point B. As shown in this figure, a well-behaved response can be obtained by selecting an appropriate truncation time, while selecting an incorrect truncation time can result in dispersion in the recorded responses. In this example, time step (dt) is considered equal to 0.0001s and 0.7 seconds of the vibration is recorded. As Figure 20 indicates, by setting the truncation time equal to 0.02s, the VUIR is calculated only for 200 steps and computational efforts of the

remaining 6800 steps are removed. This reduction can have greater impact in the long period analysis such as seismic wave propagation problems. The elapsed time of the analysis for different truncation times is plotted in Figure 21(a). This figure shows that large truncation times make the method temporally expensive (as the AUIR based scaled boundary method), while in Figure 20 it is indicated that an optimal truncation time with sufficient accuracy can be selected. Remained computational efforts in the presented method for determining the VUIR matrix can be achieved by Lehmann (2005)'s formula. This formula is written in Eq. 37. In this equation, the used parameters can be defined as: $m=t_c/dt$ and $n=T/dt$ (T=period of vibration). The reduction ratio of computational efforts can be determined by using Eq. 38.

$$o(\psi)=o(m/n)=\frac{m}{n}(2-\frac{m}{n}) \quad (37)$$

$$reduction\ \ ratio\,(\%)=1-o(\psi) \quad (38)$$

By using these equations, Figure 21(b) is plotted. As shown in this figure, the computational effort of the method can be substantially reduced by selecting an optimum truncation time (for example, $t_c=300$ for this analysis). Computational effort for the proposed method can be significantly decreased by reducing the truncation time, as shown in Figure 21(b). Choosing m=300, for example, eliminates 91% of computational effort. Therefore, selecting an appropriate truncation time in the VUIR based SBM makes the method more efficient while maintaining its accuracy.

Based on the explained results, it can be concluded that utilizing the proposed approach leads to a sufficient agreement compared with the conventional boundary element method and with the extended mesh approach. As both the BEM and the proposed VUIR based SBM are semi analytical methods, the results of these methods have almost identical accuracy, while the SBM does not require fundamental solution and consumes less computational time.

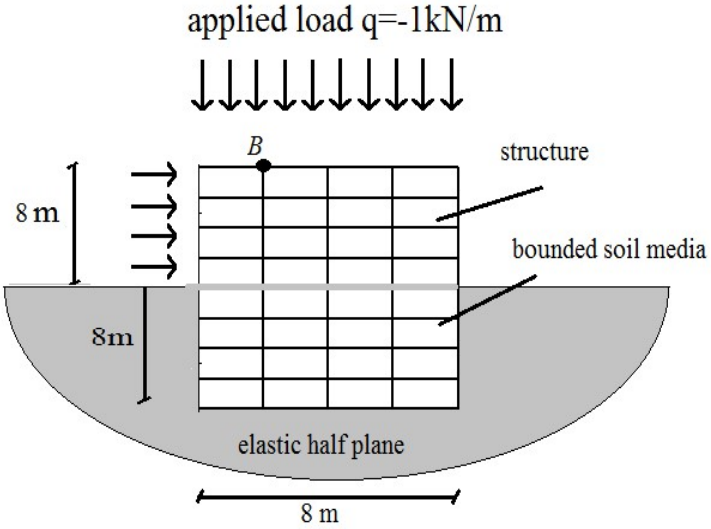

Fig. 18 Used mesh and geometry details of the considered soil structure interaction problem

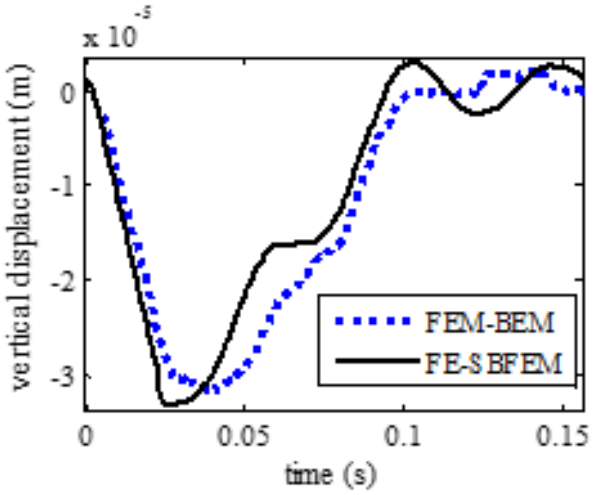

(a)

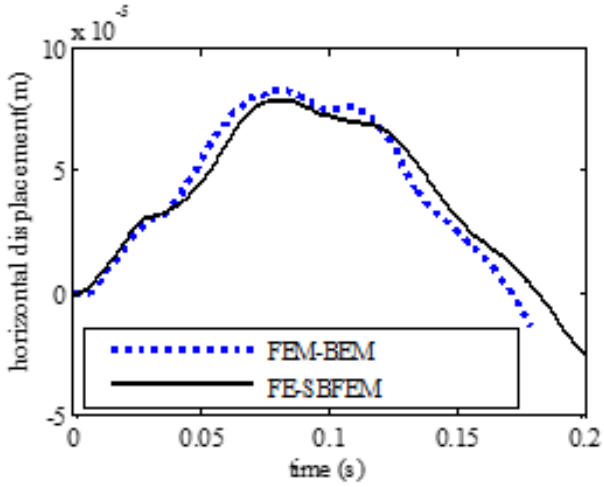

(b)

Fig. 19 (a) Horizontal displacement of point B (b) vertical displacement of point B

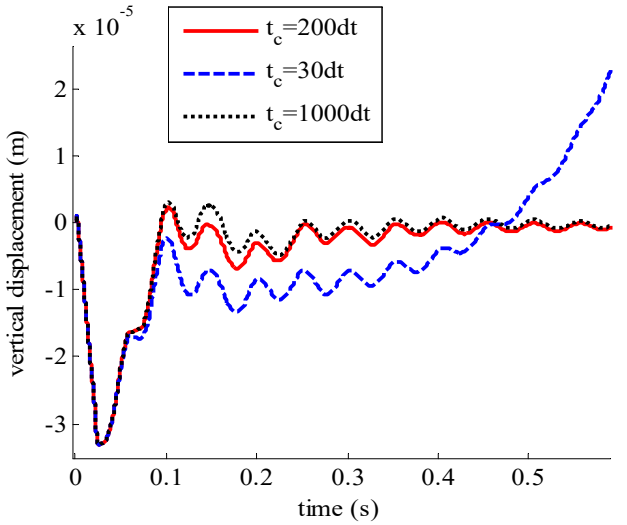

Fig. 20 Vertical displacement time history of point B by three different truncation times

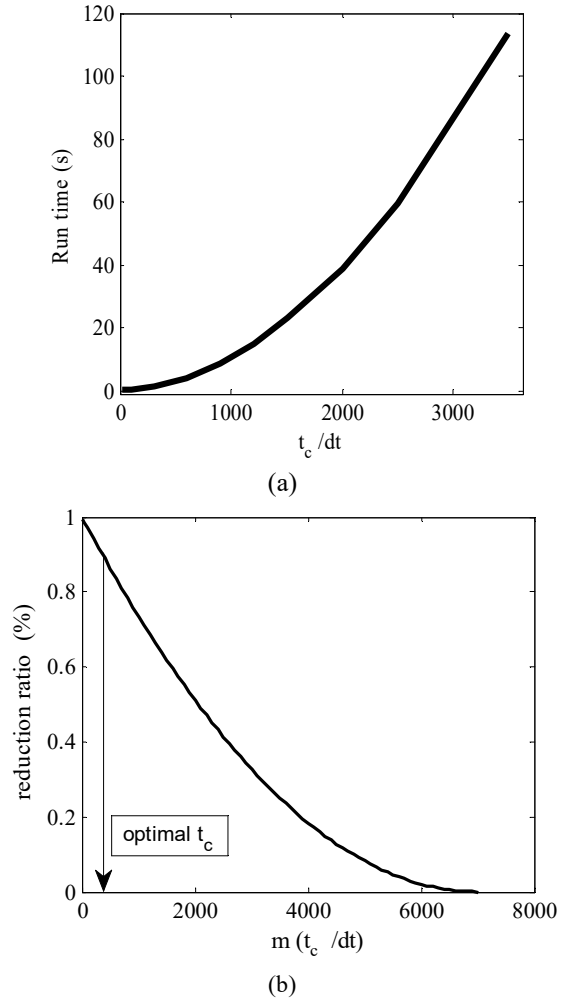

Fig. 21 (a) Run time required for computing velocity unit impulse response matrix by different truncation times, (b) reduction ratio of computational efforts by different truncation times

IV. Conclusion

The VUIR matrix-based scaled boundary equation is applied to time-domain modeling of non-homogeneous unbounded media. The variable elastic modulus and mass density are used to account for the non-homogeneity of the unbounded domain. For the sake of convenience, these parameters are regarded as power functions of spatial coordinates. A VUIR-based formulation for dynamic interaction force is developed. By evaluating various numerical problems, the precision and functionality of the presented method are assessed, and it is shown that the validated method produces reliable answers. Non-homogeneity of materials in depth and radial direction is investigated. Effects of the truncation time on the results are studied and it is indicated that by selecting an appropriate truncation time, computational efforts of the method can be reduced significantly, elapsed time in the analysis can be decreased and accurate results can be achieved.

Acknowledgment

We extend our thanks to the reviewers for their meticulous attention to detail and constructive suggestions that greatly improved the quality of this manuscript. Your contributions have been instrumental in shaping this work.

Authors' contributions

Zahra Abbaspour conducted the main data analysis, contributed to the data collection, preprocessing, and interpretation, and was responsible for drafting the initial manuscript. Kamyab Abdolnajaghi assisted in the development of the methodology and performed validation checks, provided supervision, conceptual guidance, and critical revision of the manuscript. All authors read and approved the final manuscript.

Conflict of interest

The authors have not disclosed any competing interests.

Open Access

References

Aslmand M., Kani I.M., Genes M.C. (2019). Efficient Dynamic Analysis of Foundation via a Coupled Axisymmetric SBFEM-3D FEM. *Teknik Dergi*, 30(4), 9327–9352. https://doi.org/10.18400/tekderg.447721.

Bazyar M.H., Song C. (2006a). Time-harmonic response of non-homogeneous elastic unbounded domains using the scaled boundary finite-element method. *Earthquake Engineering & Structural Dynamics*, 35(3), 357-383. https://doi.org/10.1002/eqe.526.

Bazyar M.H., Song C. (2006b). Transient analysis of wave propagation in non-homogeneous elastic unbounded domains by using the scaled boundary finite-element method. *Earthquake Engineering & Structural Dynamics*, 35(14), 1787-1806. https://doi.org/10.1002/eqe.606.

Bazyar M.H., Talebi A. (2015). Transient seepage analysis in zoned anisotropic soils based on the scaled boundary finite-element method. *International Journal for Numerical and Analytical Methods in Geomechanics*, 39(1), 1-22. https://doi.org/10.1002/nag.2291.

Birk C., Gravenkamp H., Bazyar M.H. (2017). Elastic wave radiation and scattering in heterogeneous soil using the scaled boundary finite element method. *PAMM*, 17(1), 671-672. https://doi.org/10.1002/pamm.201710304.

Chen X., Birk C., Song C. (2014). Numerical modelling of wave propagation in anisotropic soil using a displacement unit-impulse-response-based formulation of the scaled boundary finite element method. *Soil Dynamics and Earthquake Engineering*, 65, 243-255. https://doi.org/10.1016/j.soildyn.2014.06.019.

Deeks A.J., Wolf J.P. (2002). A virtual work derivation of the scaled boundary finite-element method for elastostatics. *Computational Mechanics*, 28(6), 489-504. https://doi.org/10.1007/s00466-002-0314-2.

Genes M.C., Kocak S. (2005). Dynamic soil-structure interaction analysis of layered unbounded media via a coupled finite element/ boundary element/scaled boundary finite element model. *International Journal for Numerical Methods in Engineering*, 62(6), 798-823. https://doi.org/10.1002/nme.1212.

Hajialilue-Bonab M., Tohidvand H.R. (2015). A modified scaled boundary approach in frequency domain with diagonal coefficient matrices. *Engineering Analysis with Boundary Elements*, 50, 8-18. https://doi.org/10.1016/j.enganabound.2014.07.001.

Hassanzadeh M., Tohidvand H.R., Hajialilue-Bonab M., Javadi A.A. (2018). Scaled boundary point interpolation method for seismic soil-tunnel interaction analysis. *Computers and Geotechnics*, 101, 208-216. https://doi.org/10.1016/j.compgeo.2018.05.007.

Lehmann L. (2005). An effective finite element approach for soil-structure analysis in the time-domain. *Structural Engineering and Mechanics*, 21(4), 437-450. https://doi.org/10.12989/sem.2005.21.4.437.

Lin G., Zhang Y., Hu Z., Zhong H. (2014). Scaled boundary isogeometric analysis for 2D elastostatics. *Science China Physics, Mechanics and Astronomy*, 57(2), 286-300. https://doi.org/10.1007/s11433-013-5146-x.

Pak R.Y.S., Guzina B.B. (1999). Seismic soil-structure interaction analysis by direct boundary element methods. *International Journal of Solids and Structures*, 36(31-32), 4743-4766. https://doi.org/10.1016/S0020-7683(98)00263-7.

Rafiezadeh K., Ataie-Ashtiani B. (2012). Three dimensional flow in anisotropic zoned porous media using boundary element method. *Engineering Analysis with Boundary Elements*, 36(5), 812-824. https://doi.org/10.1016/j.enganabound.2011.12.002.

Rahnema H., Mohasseb S., JavidSharifi B. (2016). 2D soil-structure interaction in time domain by the SBFEM and two non-linear soil models. *Soil Dynamics and Earthquake Engineering*, 88, 152-175. https://doi.org/10.1016/j.soildyn.2016.01.008.

Ribeiro D.B., de-Paiva J.B. (2014). A new BE formulation coupled to the FEM for simulating vertical pile groups. *Engineering Analysis with Boundary Elements*, 41, 1-9. https://doi.org/10.1016/j.enganabound.2014.01.007.

Syed N.M., Maheshwari B.K. (2015). Improvement in the computational efficiency of the coupled FEM-SBFEM approach for 3D seismic SSI analysis in the time domain. *Computers and Geotechnics*, 67, 204-212. https://doi.org/10.1016/j.compgeo.2015.03.010.

Von Estorff O., Firuziaan M. (2000). *Engineering Analysis with Boundary Elements*, 24(10), 715-725.https://doi.org/10.1016/S0955-7997(00)00054-0.

Wolf J.P. (2003). *The scaled boundary finite element method*. John Wiley & Sons, Chichester, England, UK.

Wolf J.P., Song C. (1996), *Finite-element modelling of unbounded media*. Wiley, Chichester, England, UK.

Yaseri A., Bazyar M., Hataf N. (2014). 3D coupled scaled boundary finite-element/finiteelement analysis of ground vibrations induced by underground train movement. *Computers and Geotechnics*, 60, 1-8. https://doi.org/10.1016/j.compgeo.2014.03.013.

Yazdchi M., Khalili N., Valliappan S. (1999). Dynamic soil–structure interaction analysis via coupled finite element boundary element method. *Soil Dynamics and Earthquake Engineering*, 1999, 18(7), 499-517. https://doi.org/10.1016/S0267-7261(99)00019-6.